Article

Journal of Vibration and Control
2016, Vol. 22(7) 1889–1894

DOI: 10.1177/1077546314546511
jvc.sagepub.com
SAGE

A note on elastic noise source localization

Abdul Wahab and Rab Nawaz

Abstract

The problem of reconstructing the spatial support of ambient noise sources from elastic wavefield boundary measurements using cross-correlation techniques is dealt with. It is demystified that the cross-correlation-based standard source localization functional in elastic media does not provide optimal refocusing due to different pressure and shear wave speeds. Then, a weighted functional is proposed to rectify the coupling artifacts. A numerical experiment is presented to substantiate the appositeness of the proposed functional.

Keywords

Noise source localization, elasticity imaging, inverse source problem

1. Introduction

We consider the problem of reconstructing the spatial support of ambient noise sources from boundary wavefield measurements in an isotropic homogeneous elastic medium in two or three dimensions using cross-correlation techniques (Borcea et al., 2010; Garnier and Papanicolaou, 2012; Garnier et al., 2013; Hoop et al., 2013). The main application envisaged for the present work is so-called *passive elastography* where the aim is to identify the *muscle noise sources* in an isotropic elastic medium (Gennisson et al., 2003; Sabra et al., 2007; Archer and Sabra, 2010; Carmona, 2011; Ammari et al., 2014). Another potential application is the localization of the Earth's background noise source distribution, which contains significant information about the regional geology, time-dependent crustal changes and earthquakes (Asghar et al., 1998; Garnier and Papanicolaou, 2009; Kader, 2011; Hoop et al., 2013; Nawaz and Lawrie, 2013). Nayfeh (1995), Chen et al. (2008), Kuske (2010), Shen et al. (2013), Afzal et al. (2014) and Nawaz et al. (2014) detail other potential applications and techniques associated with the present work.

The problem of ambient noise source localization in acoustic media (both attenuating and nonattenuating) has been considered by Ammari et al. (2012) wherein cross-correlation-based imaging functionals were established. In this note, we extend the same approach to elastic media. We first consider the elastic counterpart of the source localization functional used by Ammari et al. (2012). Unfortunately, it mixes the irrotational and solenoidal components of the source due to different pressure and shear wave speeds. Nevertheless, we present a new weighted functional, based on a Helmholtz decomposition for the Green function (initially proposed by Ammari et al. (2013)), taking into account the different wave speeds for pressure and shear waves.

2. Mathematical formulation

Let $\Omega \subset \mathbb{R}^d$, $d=2,3$, be an open bounded domain, occupied by a homogeneous isotropic elastic material, with Lipschitz boundary $\partial\Omega$.

Consider the linear elastic wave equation in $\mathbb{R}^d$, that is

$$\begin{cases} \dfrac{\partial^2 \mathbf{u}}{\partial t^2}(\mathbf{x},t) - \mathcal{L}_{\lambda,\mu}\mathbf{u}(\mathbf{x},t) = \mathbf{n}(\mathbf{x},t), & t \in \mathbb{R}, \\ \mathbf{u}(\mathbf{x},t) = \dfrac{\partial \mathbf{u}}{\partial t}(\mathbf{x},t) = \mathbf{0}, \ \mathbf{x} \in \mathbb{R}^d, & t \ll 0 \end{cases} \tag{1}$$

for all $\mathbf{x} \in \mathbb{R}^d$ where

$$\mathcal{L}_{\lambda,\mu}\mathbf{u} = \mu\Delta\mathbf{u} + (\lambda+\mu)\nabla(\nabla\cdot\mathbf{u}) \tag{2}$$

Department of Mathematics, COMSATS Institute of Information Technology, Pakistan

Received: 10 March 2014; accepted: 8 July 2014

Corresponding author:
Rab Nawaz, Department of Mathematics, COMSATS Institute of Information Technology, 47040, Wah Cantt., Pakistan.
Email: rabnawaz@ciitwah.edu.pk

Here (λ, μ) are the Lamé coefficients of Ω and its density is assumed to be constant and is taken as one without loss of generality. The term $\mathbf{n}(\mathbf{x}, t)$ models a distribution of noise sources that is compactly supported in domain Ω. Furthermore, we assume that $\mathbf{n}(\mathbf{x}, t)$ is a stationary (in time) Gaussian process with the mean zero and covariance function

$$\left\langle \mathbf{n}(\mathbf{x}, t)\mathbf{n}^{\dagger}(\mathbf{y}, s)\right\rangle = F(t-s)\mathbb{K}(\mathbf{x})\delta(\mathbf{x}-\mathbf{y}) \tag{3}$$

where δ is the Dirac mass at the origin, the brackets stand for statistical average, $\dagger$ indicates a transpose operation and F is the time covariance of noise signals (its Fourier transform is the power spectral density). The quantity of interest $\mathbb{K}$ is a symmetric matrix, that characterizes the spatial support of the sources. We aim to identify $\mathbb{K}$ using the data set

$$\left\{\mathbf{u}(\mathbf{x}, t),\ \forall t \in [0, T], \mathbf{x} \in \partial\Omega\right\}$$

for sufficiently large T.

Let $\widehat{\mathbb{G}}$ be the fundamental solution, subject to the outgoing Sommerfeld–Kupradze radiation condition, to the time-harmonic elastic wave equation

$$(\mathcal{L}_{\lambda,\mu} + \omega^2)\widehat{\mathbb{G}}(\mathbf{x}, \mathbf{y}, \omega) = -\delta(\mathbf{x}-\mathbf{y})\mathbb{I} \quad \text{in } \mathbb{R}^d$$

We recall, for instance from Aki and Richards (1980) and Ammari (2008), that $\widehat{\mathbb{G}}(\mathbf{x}, \mathbf{y}, \omega)$ can be expressed in the form

$$\widehat{\mathbb{G}}(\mathbf{x}, \mathbf{y}, \omega) = \frac{1}{\mu\kappa_s^2}\left(\kappa_s^2 g^s(\mathbf{x}, \mathbf{y}, \omega)\mathbb{I} + \mathbb{D}(g^s - g^p)(\mathbf{x}, \mathbf{y}, \omega)\right) \tag{4}$$

for all $\mathbf{x},\mathbf{y} \in \mathbb{R}^d$ such that $\mathbf{x} \neq \mathbf{y}$, where

$$\mathbb{I} = \left(\delta_{ij}\right)_{i,j=1}^{d}, \quad \mathbb{D} = \left(\partial x_i \partial x_j\right)_{i,j=1}^{d}$$

and

$$\kappa_s^2 = \frac{\omega^2}{\mu} = \frac{\omega^2}{c_s^2} \quad \kappa_p^2 = \frac{\omega^2}{\lambda + 2\mu} = \frac{\omega^2}{c_p^2}$$

Here, $g^{\alpha}(\mathbf{x},\mathbf{y},\omega)$ is the outgoing fundamental solution to the Helmholtz operator $-(\Delta + \kappa_{\alpha}^2)$ in $\mathbb{R}^d$ with $\alpha = p,s$.

We observe the waves at surface $\partial\Omega$ over the time interval $[0,T]$ and compute the empirical cross-correlation

$$\mathbb{C}_T(\mathbf{x}, \mathbf{y}, \tau) = \frac{1}{T}\int_0^{\mathrm{T}} \mathbf{u}(\mathbf{x}, t)\mathbf{u}^{\dagger}(\mathbf{y}, t+\tau)\,\mathrm{d}t \tag{5}$$

for all $\mathbf{x},\mathbf{y} \in \partial\Omega$. If the recording time window is long enough then the empirical cross-correlation is equivalent to the statistical cross-correlation (Garnier and Papanicolaou, 2009)

$$\begin{aligned}\mathbb{C}(\mathbf{x}, \mathbf{y}, \tau) = &< \mathbf{u}(\mathbf{x}, t)\mathbf{u}^{\dagger}(\mathbf{y}, t+\tau) > \\ &= \frac{1}{2\pi}\int_{\mathbb{R}}\int_{\Omega} \overline{\widehat{\mathbb{G}}(\mathbf{x}, \mathbf{z}, \omega)}\mathbb{K}(\mathbf{z})\widehat{\mathbb{G}}^{\dagger}(\mathbf{y}, \mathbf{z}, \omega) \\ &\quad \widehat{F}(\omega)e^{-i\omega\tau}\,\mathrm{d}\mathbf{z}\,\mathrm{d}\omega\end{aligned} \tag{6}$$

where $\mathbb{C}$ contains all the information about the data. Indeed the data set has a stationary Gaussian distribution with mean zero, so that its statistical distribution is fully characterized by the cross-correlation (Garnier and Papanicolaou, 2009; Carmona, 2011). Here the superposed bar indicates complex conjugation.

3. Helmholtz decomposition of fundamental solution

In the sequel, we decompose fundamental solution $\widehat{\mathbb{G}}$ into the sum of an irrotational field $\widehat{\mathbb{G}}^p$ and a solenoidal field $\widehat{\mathbb{G}}^s$. We will need the following Hilbert spaces

$$\begin{aligned}H^1(\Omega) &= \left\{v \in L^2(\Omega) :\ \nabla v \in L^2(\Omega)\right\}, \\ H_{\mathrm{curl}}(\Omega) &= \left\{\mathbf{v} \in L^2(\Omega)^d :\ \nabla \times \mathbf{v} \in L^2(\Omega)^d\right\}, \\ H_{\mathrm{div}}(\Omega) &= \left\{\mathbf{v} \in L^2(\Omega)^d :\ \nabla \cdot \mathbf{v} \in L^2(\Omega)\right\}\end{aligned}$$

equipped with the norms

$$\begin{aligned}\|v\|_{H^1(\Omega)} &:= \sqrt{\int_{\Omega}\left[|v|^2 + |\nabla v|^2\right]\mathrm{d}\mathbf{x}}, \\ \|\mathbf{v}\|_{H_{\mathrm{curl}}(\Omega)} &:= \sqrt{\int_{\Omega}\left[|\mathbf{v}|^2 + |\nabla \times \mathbf{v}|^2\right]\mathrm{d}\mathbf{x}}, \\ \|\mathbf{v}\|_{H_{\mathrm{div}}(\Omega)} &:= \sqrt{\int_{\Omega}\left[|\mathbf{v}|^2 + |\nabla \cdot \mathbf{v}|^2\right]\mathrm{d}\mathbf{x}}\end{aligned}$$

Assume that Ω is simply connected, homogeneous and isotropic with the connected boundary $\partial\Omega$. Then Helmholtz decomposition states that for $\mathbf{v} \in L^2(\Omega)^d$, there exist $\phi_{\mathbf{v}} \in H^1(\Omega)$ and $\psi_{\mathbf{v}} \in H_{\mathrm{curl}}(\Omega) \cap H_{\mathrm{div}}(\Omega)$ such that

$$\mathbf{v} = \nabla\phi_{\mathbf{v}} + \nabla \times \psi_{\mathbf{v}} \tag{7}$$

where $\phi_{\mathbf{v}}$ solves the weak Neumann problem

$$\int_{\Omega} \nabla\phi_{\mathbf{v}} \cdot \nabla p\,\mathrm{d}\mathbf{x} = \int_{\Omega} \mathbf{v} \cdot \nabla p\,\mathrm{d}\mathbf{x}, \quad \forall p \in H^1(\Omega) \tag{8}$$

and is unique up to an additive constant. In order to fix the constant and to uniquely determine the

corresponding $\psi_{\mathbf{v}}$, we enforce the following properties (Borchers and Sohr, 1990; Galdi, 1994)

$$\begin{cases} \nabla \cdot \psi_{\mathbf{v}} = 0 & \text{in } \Omega, \\ \psi_{\mathbf{v}} \cdot \nu = (\nabla \times \psi_{\mathbf{v}}) \cdot \nu & \text{on } \partial\Omega \end{cases} \tag{9}$$

where ν is the outward unit normal to $\partial\Omega$. The boundary condition

$$(\nabla \times \psi_{\mathbf{v}}) \cdot \nu = 0 \quad \text{on} \quad \partial\Omega$$

shows that the divergence-free and rotation-free parts in equation (7) are orthogonal. We define, respectively, the decomposition operators $\mathcal{H}^p$ and $\mathcal{H}^s$ for $\mathbf{v} \in L^2(\Omega)^d$ by

$$\mathcal{H}^p[\mathbf{v}] := \nabla\phi_{\mathbf{v}} \quad \text{and} \quad \mathcal{H}^s[\mathbf{v}] := \nabla \times \mathbf{v}$$

where $\phi_{\mathbf{v}}$ is a solution to equation (8) and $\psi_{\mathbf{v}}$ satisfies

$$\nabla \times \psi_{\mathbf{v}} = \mathbf{v} - \nabla\phi_{\mathbf{v}}$$

together with equation (9). The L^2-projectors $\mathcal{H}^p$ and $\mathcal{H}^s$ are pseudo-differential operators with kernels $\pi_p(\mathbf{x},\xi)$ equal to the orthogonal projector onto $\mathbb{R}\xi$ and $\pi_s = \mathrm{I} - \pi_p$ respectively; see, for instance, Schwarz, (1995). Therefore, $\widehat{\mathbb{G}}$ can be decomposed as

$$\widehat{\mathbb{G}} = \widehat{\mathbb{G}}^p + \widehat{\mathbb{G}}^s \tag{10}$$

with

$$\widehat{\mathbb{G}}^p = \mathcal{H}^p[\widehat{\mathbb{G}}] \quad \text{and} \quad \widehat{\mathbb{G}}^s = \mathcal{H}^s[\widehat{\mathbb{G}}] \tag{11}$$

where $\mathcal{H}^\alpha[\widehat{\mathbb{G}}]$ signifies that

$$\mathcal{H}^\alpha[\widehat{\mathbb{G}}]\mathbf{q} = \mathcal{H}^\alpha[\widehat{\mathbb{G}}\mathbf{q}], \quad \forall \mathbf{q} \in \mathbb{R}^d, \ \alpha = p, s \tag{12}$$

Finally, we define the weighted fundamental solutions $\widehat{\mathbf{\Gamma}}$ by

$$\widehat{\mathbf{\Gamma}}(\mathbf{x}, \mathbf{y}, \omega) = c_s \widehat{\mathbb{G}}^s(\mathbf{x}, \mathbf{y}, \omega) + c_p \widehat{\mathbb{G}}^p(\mathbf{x}, \mathbf{y}, \omega) \tag{13}$$

4. Source localization

We aim to identify the source matrix $\mathbb{K}$. The idea is to back-propagate the cross-correlation of the data, which contains all the accessible information about the source distribution. Consider the source localization functional, which is an elastic counterpart of the one proposed by Ammari et al. (2012), given by

$$\begin{aligned} \mathcal{I}(\mathbf{z}^S) &= 2\pi \int\int\int\int_{\partial\Omega\times\partial\Omega\times\mathbb{R}^+\times\mathbb{R}^+} \mathbb{G}^\dagger(\mathbf{x}, \mathbf{z}^S, t) \\ &\quad \mathbb{C}(\mathbf{x}, \mathbf{y}, s-t)\mathbb{G}(\mathbf{y}, \mathbf{z}^S, s)\, \mathrm{d}t\, \mathrm{d}s\, \mathrm{d}\sigma(\mathbf{x})\, \mathrm{d}\sigma(\mathbf{y}) \\ &= \int\int\int_{\mathbb{R}\times\partial\Omega\times\partial\Omega} \widehat{\mathbb{G}}^\dagger(\mathbf{x}, \mathbf{z}^S, \omega) \\ &\quad \widehat{\mathbb{C}}(\mathbf{x}, \mathbf{y}, \omega)\overline{\widehat{\mathbb{G}}(\mathbf{y}, \mathbf{z}^S, \omega)}\, \mathrm{d}\sigma(\mathbf{x})\, \mathrm{d}\sigma(\mathbf{y})\, \mathrm{d}\omega \end{aligned} \tag{14}$$

for the search point $\mathbf{z}^S \in \Omega$. Here $\widehat{\mathbb{C}}$ is the Fourier transform of $\mathbb{C}$ defined by equation (6) and $\mathrm{d}\sigma$ is the surface element on $\partial\Omega$. The following elastic identities, from Ammari et al. (2013), play a vital role in further discussion.

Lemma 1. (Helmholtz–Kirchhoff identities). *In a homogeneous isotropic elastic medium, we have for all* $\mathbf{x}, \mathbf{z} \in \Omega$ *sufficiently far from* $\partial\Omega$ *(with respect to wavelength)*

$$\Re e\left\{\int_{\partial\Omega} \widehat{\mathbb{G}}^s(\mathbf{x}, \mathbf{y}, \omega)\overline{\widehat{\mathbb{G}}^p(\mathbf{y}, \mathbf{z}, \omega)}\, \mathrm{d}\sigma(\mathbf{y})\right\} \simeq 0, \tag{15}$$

$$\begin{aligned} &\Re e\left\{\int_{\partial\Omega} \widehat{\mathbb{G}}^\alpha(\mathbf{x}, \mathbf{y}, \omega)\overline{\widehat{\mathbb{G}}^\alpha(\mathbf{y}, \mathbf{z}, \omega)}\, \mathrm{d}\sigma(\mathbf{y})\right\} \\ &\quad \simeq \frac{1}{\omega c_\alpha} \Im m\left\{\widehat{\mathbb{G}}^\alpha(\mathbf{x}, \mathbf{z}, \omega)\right\} \end{aligned} \tag{16}$$

where $\alpha = p, s$, $c_s = \sqrt{\mu}$ *and* $c_p = \sqrt{\lambda + 2\mu}$ *are shear and pressure wave speeds.*

As a consequence, we have the following result.

Proposition 2. *The imaging functional* $\mathcal{I}(\mathbf{z}^S)$, *defined by equation* (14), *mixes the components of the support matrix* $\mathbb{K}$. *Precisely*

$$\mathcal{I}(\mathbf{z}^S) \simeq \int_\Omega \mathcal{Q}(\mathbf{z}^S, \mathbf{z})\mathbb{K}(\mathbf{z})\, \mathrm{d}\mathbf{z} \tag{17}$$

with the kernel $\mathcal{Q}$ *defined by*

$$\begin{aligned} \mathcal{Q}(\mathbf{z}^S, \mathbf{z}) &:= \int_{\mathbb{R}} \frac{\widehat{F}(\omega)}{\omega^2} \\ &\left(\frac{c_s + c_p}{2c_s c_p} \Im m\left\{\widehat{\mathbb{G}}(\mathbf{z}^S, \mathbf{z}, \omega)\right\} + \frac{c_s - c_p}{2c_s c_p} \mathbb{B}(\mathbf{z}^S, \mathbf{z}, \omega)\right)^2 \mathrm{d}\omega \end{aligned} \tag{18}$$

where the matrix $\mathbb{B}$, *given by*

$$\mathbb{B}(\mathbf{x}, \mathbf{y}, \omega) = \Im m\left\{(\widehat{\mathbb{G}}^p - \widehat{\mathbb{G}}^s)\right\}(\mathbf{x}, \mathbf{y}, \omega)$$

is nondiagonal and characterizes the error whenever $c_s \neq c_p$.

Thus, the elastic counterpart $\mathcal{I}(\mathbf{z}^S)$ of the acoustic imaging functional (Ammari et al., 2012) does not provide the ideal source localization in elastic media. Indeed, the measured field at the surface $\partial\Omega$ has nonlinearly coupled pressure and shear wave components. Consequently, the back-propagation of these signals introduces the interference of the components of $\mathbb{K}(x)$

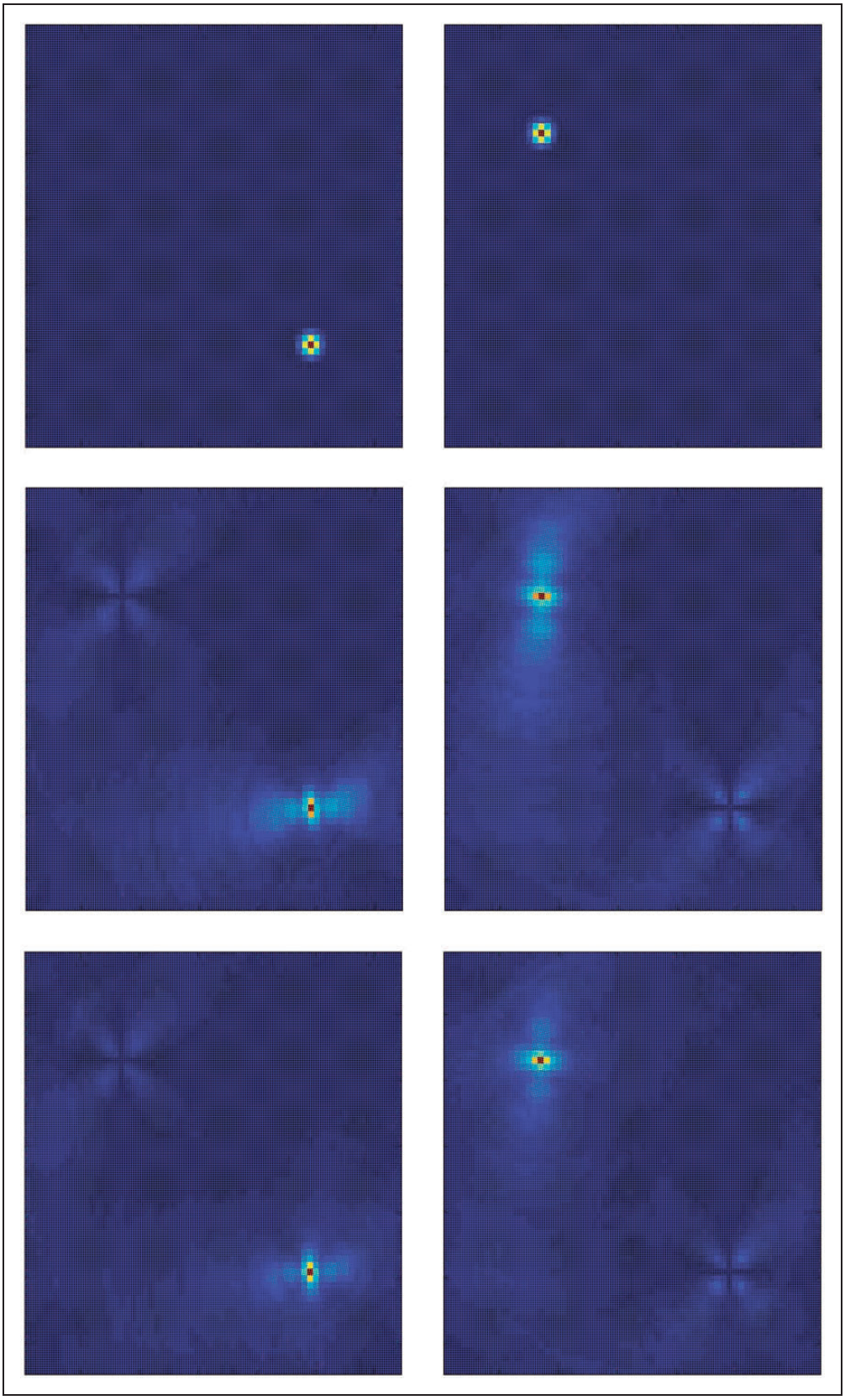

Figure 1. Comparison between $\mathcal{I}$ and $\widetilde{\mathcal{I}}$ in an elastic medium. The Lamé parameters are $(\lambda,\mu) = (10,1)$. Left: pressure component $\mathcal{H}^P[\mathbb{K}]$, right: shear component $\mathcal{H}^S[\mathbb{K}]$. Top to bottom: initial source $\mathbf{n}$; reconstruction of $\mathcal{I}$ and $\widetilde{\mathcal{I}}$.

because of different wave speeds. Unfortunately, the components of the boundary measurements cannot be uncoupled using Helmholtz decomposition without extrapolating the measurements into a neighborhood of $\partial\Omega$, which is neither practical nor apt. To take into account the wave speed discrepancy in back-propagation, we define a modified weighted imaging functional

$$\widetilde{\mathcal{I}}(\mathbf{z}^S) := \int\int\int_{\mathbb{R}\times\partial\Omega\times\partial\Omega} \widehat{\mathbf{\Gamma}}^{\dagger}(\mathbf{x},\mathbf{z}^S,\omega)\widehat{\mathbb{C}}(\mathbf{x},\mathbf{y},\omega)\overline{\widehat{\mathbf{\Gamma}}(\mathbf{y},\mathbf{z}^S,\omega)}\, d\sigma(\mathbf{x})\, d\sigma(\mathbf{y})\, d\omega \tag{19}$$

where $\widehat{\mathbf{\Gamma}}$ is defined in equation (13).

As an immediate consequence of Lemma 1, the following result holds.

Theorem 3. *The imaging functional $\widetilde{\mathcal{I}}$, defined by equation* (19)*, gives the support function $\mathbb{K}$ up to a smoothing operator $\mathcal{Q}$, that is*

$$\widetilde{\mathcal{I}}(\mathbf{z}^S) \simeq \int_{\Omega} \widetilde{\mathcal{Q}}(\mathbf{z}^S,\mathbf{z})\mathbb{K}(\mathbf{z})\, d\mathbf{z} \tag{20}$$

with

$$\widetilde{\mathcal{Q}}(\mathbf{z}^S,\mathbf{z}) = \int_{\mathbb{R}} \frac{\widehat{F}(\omega)}{\omega^2} \Im m\left\{\widehat{\mathbb{G}}(\mathbf{z}^S,\mathbf{z},\omega)\right\}^2 d\omega \tag{21}$$

In view of Theorem 3, the resolution of the imaging functional $\widetilde{\mathcal{I}}$ is determined by the kernel $\widetilde{\mathcal{Q}}(\mathbf{z}^S,\mathbf{z})$. The high-frequency components are penalized in this functional because of the factor ω^{-2} and therefore, the resolution is still limited. In order to achieve better resolution, one can further modify the imaging functional to make its smoothing kernel as close as possible to a Dirac distribution $\delta(\mathbf{z}^S-\mathbf{z})$ thereby enhancing the high frequencies. However, one should be aware that enhancing the high-frequency components may cause instability in the imaging procedure. To this end, an imaging functional where the weights are chosen in terms of the power spectral density of the noise source can be established using analogous, but more involved, arguments, as in Ammari et al. (2012).

We present a numerical experiment to illustrate the performance of the two imaging functionals in Figure 1. The irrotational and solenoidal components of the source matrix are plotted along with their reconstructions using $\mathcal{I}$ and $\widetilde{\mathcal{I}}$. The side-lobes indicating the coupling of the shear and pressure components of the source matrix are apparent in the reconstructed images obtained using $\mathcal{I}$. On the other hand, $\widetilde{\mathcal{I}}$ clearly produces very small side-lobes around the source location compared to $\mathcal{I}$, substantiating the appositeness of the proposed imaging functional.

5. Conclusion

In this note, we have discussed two imaging functions for reconstructing ambient noise sources in an elastic medium using cross-correlations. We substantiated that the standard source localization functional couples the shear and pressure components of the source and provides an imaging functional based on weighted Helmholtz decomposition to counter these coupling artifacts. The weighed imaging functions, with weights depending on power spectral density, will be presented in a forthcoming work. The cases of inhomogeneous media and spatially correlated sources will also be taken into account.

Funding

This research received no specific grant from any funding agency in the public, commercial, or not-for-profit sectors.

References

Afzal M, Nawaz R, Ayub M and Wahab A (2014) Acoustic scattering in flexible waveguide involving step discontinuity. *PLoS One* 9(8): e103807. DOI:10.1371/journal.pone.0103807.

Aki K and Richards PG (1980) *Quantitative Seismology*. San Francisco: Freeman and Co.

Ammari H (2008) *An Introduction to Mathematics of Emerging Biomedical Imaging*. Berlin: Springer-Verlag.

Ammari H, Bretin E, Garnier J and Wahab A (2012) Noise source localization in an attenuating acoustic medium. *SIAM Journal on Applied Mathematics* 72: 317–336.

Ammari H, Bretin E, Garnier J and Wahab A (2013) Time reversal algorithms for viscoelastic media. *European Journal of Applied Mathematics* 24: 565–600.

Ammari H, Bretin E, Garnier J, Kang H, Lee H and Wahab A (2014) *Mathematical Methods in Elasticity Imaging*. New Jersey: Princeton University Press.

Archer A and Sabra KG (2010) Two dimensional spatial coherence of the natural vibrations of the biceps brachii muscle generated during voluntary contractions. In: *IEEE Engineering in Medicine & Biology Society (EMBC'10)*, Buenos Aires, Argentina, 31 August – 4 September 2010, pp. 170–173. Piscataway: IEEE Press.

Asghar S, Hayat T, Ayub M and Ahmad B (1998) Scattering of a spherical Gaussian pulse near an absorbing half plane. *Applied Acoustics* 54: 323–338.

Borcea L, Issa L and Tsogka C (2010) Source localization in random acoustic waveguides. *Multiscale Modeling & Simulation* 8: 1981–2022.

Borchers W and Sohr H (1990) On the equations rot $v=g$ and div $u=f$ with zero boundary conditions. *Hokkaido Mathematical Journal* 19: 67–87.

Carmona M (2011) *Identification passive des milieux de propagation élastiques*. PhD Thesis, Université de Grenoble, France.

Chen Y, Sun R, Zhou A and Zaveri N (2008) Fractional order signal processing of electrochemical noises. *Journal of Vibration and Control* 14: 1443–1456.

Galdi GP (1994) *An Introduction to the Mathematical Theory of the Navier–Stokes Equations I: Linearized Steady Problems*. New York: Springer-Verlag.

Garnier J and Papanicolaou G (2009) Passive sensor imaging using cross correlations of noisy signals in a scattering medium. *SIAM Journal on Imaging Sciences* 2: 396–437.

Garnier J and Papanicolaou G (2012) Correlation-based virtual source imaging in strongly scattering random media. *Inverse Problems* 28: 075002.

Garnier J, Papanicolaou G, Semin A and Tsogka C (2013) Signal-to-noise ratio estimation in passive correlation-based imaging. *SIAM Journal on Imaging Sciences* 6: 1092–1110.

Gennisson JL, Catheline S, Chaffai S and Fink M (2003) Transient elastography in anisotropic medium: Application to the measurement of slow and fast shear wave speeds in muscles. *Journal of the Acoustical Society of America* 114: 536–541.

Hoop MV, Garnier J, Holman SF and Sølna K (2013) Retrieval of a Green's function from partly coherent waves generated by a wave packet using cross correlations. *SIAM Journal on Applied Mathematics* 73: 493–522.

Kader S (2011) Source distribution of ocean microseisms and implications for time-dependent noise tomography. *Comptes Rendus Geoscience* 343: 548–557.

Kuske R (2010) Competition of noise sources in systems with delay: The role of multiple time scales. *Journal of Vibration and Control* 16: 983–1003.

Nawaz R and Lawrie JB (2013) Scattering of a fluid structure coupled wave at a flanged junction between two flexible waveguids. *Journal of the Acoustical Society of America* 134: 1939–149.

Nawaz R, Wahab A and Rasheed A (2014) An intermediate range solution to a diffraction problem with impedance conditions. *Journal of Modern Optics*. Epub ahead of print 24 June 2014. DOI: 10.1080/09500340.2014.931477.

Nayfeh AH (1995) On direct methods for constructing nonlinear normal modes of continuous systems. *Journal of Vibration and Control* 1: 389–430.

Sabra KG, Conti S, Roux P and Kuperman WA (2007) Passive *in vivo* elastography from skeletal muscle noise. *Applied Physics Letters* 90: 194101.

Schwarz G (1995) *Hodge Decomposition—A Method for Solving Boundary Value Problems*. Berlin: Springer-Verlag.

Shen M, Nagamura K, Nakagawa N and Okamura M (2013) Noise reduction through elastically restrained sandwich polycarbonate window pane into rectangular cavity. *Journal of Vibration and Control* 19: 415–428.